



Dust aerosol impact on North Africa climate: a GCM investigation of aerosol-cloud-radiation interactions using A-Train satellite data

Y. Gu¹, K. N. Liou¹, J. H. Jiang^{1,2}, H. Su^{1,2}, and X. Liu³

¹Joint Institute for Regional Earth System Science and Engineering and Department of Atmospheric and Oceanic Sciences, University of California, Los Angeles, CA, USA

²Jet Propulsion Laboratory, California Institute of Technology, Pasadena, CA, USA

³Pacific Northwest National Laboratory, Richland, WA, USA

Correspondence to: Y. Gu (gu@atmos.ucla.edu)

Received: 28 October 2011 – Published in Atmos. Chem. Phys. Discuss.: 1 December 2011

Revised: 30 January 2012 – Accepted: 2 February 2012 – Published: 15 February 2012

Abstract. The climatic effects of dust aerosols in North Africa have been investigated using the atmospheric general circulation model (AGCM) developed at the University of California, Los Angeles (UCLA). The model includes an efficient and physically based radiation parameterization scheme developed specifically for application to clouds and aerosols. Parameterization of the effective ice particle size in association with the aerosol first indirect effect based on ice cloud and aerosol data retrieved from A-Train satellite observations have been employed in climate model simulations. Offline simulations reveal that the direct solar, IR, and net forcings by dust aerosols at the top of the atmosphere (TOA) generally increase with increasing aerosol optical depth. When the dust semi-direct effect is included with the presence of ice clouds, positive IR radiative forcing is enhanced since ice clouds trap substantial IR radiation, while the positive solar forcing with dust aerosols alone has been changed to negative values due to the strong reflection of solar radiation by clouds, indicating that cloud forcing associated with aerosol semi-direct effect could exceed direct aerosol forcing. With the aerosol first indirect effect, the net cloud forcing is generally reduced in the case for an ice water path (IWP) larger than 20 g m^{-2} . The magnitude of the reduction increases with IWP.

AGCM simulations show that the reduced ice crystal mean effective size due to the aerosol first indirect effect results in less OLR and net solar flux at TOA over the cloudy area of

the North Africa region because ice clouds with smaller size trap more IR radiation and reflect more solar radiation. The precipitation in the same area, however, increases due to the aerosol indirect effect on ice clouds, corresponding to the enhanced convection as indicated by reduced OLR. Adding the aerosol direct effect into the model simulation reduces the precipitation in the normal rainfall band over North Africa, where precipitation is shifted to the south and the northeast produced by the absorption of sunlight and the subsequent heating of the air column by dust particles. As a result, rainfall is drawn further inland to the northeast.

This study represents the first attempt to quantify the climate impact of the aerosol indirect effect using a GCM in connection with A-Train satellite data. The parameterization for the aerosol first indirect effect developed in this study can be readily employed for application to other GCMs.

1 Introduction

The recent Sahel drought has been recognized as one of the largest climate changes in recent history by the climate research community. Possible causes have been generally attributed to either land-atmosphere interactions (e.g., Xue and Shukla, 1993; Xue, 1997; Clark et al., 2001; Taylor et al., 2002) or the sea surface temperature (SST) contrast between Atlantic Oceans in the Northern and Southern Hemispheres

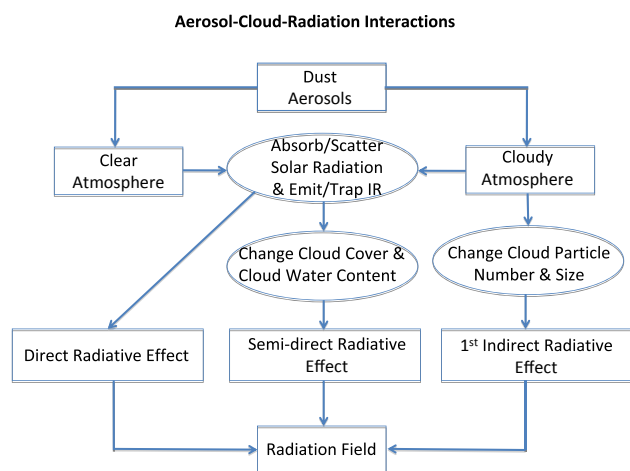


Fig. 1. Flow chart of aerosol-cloud-radiation interactions.

(e.g., Lamb and Pepler, 1992; Rowell et al., 1995; Hoerling et al., 2006). However, several studies have shown that dust can play an important role in the changes of Sahel climate (e.g., Nicholson, 2000; Prospero and Lamb, 2003; Yoshioka and Mahowald, 2007; Kim et al., 2010; Zhao et al., 2011). Dust particles play a fundamental role in the energy balance of the Earth-atmospheric system due to their high emission rate (Andreae, 1995; Satheesh and Moorthy, 2005; IPCC, 2007), entering the atmosphere through wind erosion of dry soils. North Africa is heavily influenced by dust with significant year-round dust emissions as shown in the observations derived from the Total Ozone Mapping Spectrometer (TOMS) aerosol index (AI), with maximum emissions from May to August (Engelstaedter et al., 2006). During boreal spring and summer, the air over North Africa is almost permanently loaded with significant amounts of dust.

Atmospheric aerosols generally affect global and regional climate through the scattering and absorption of solar radiation (direct effect) and through their influence on cloud formation and hence the radiation field (first indirect effect). Figure 1 illustrates the interactions among dust aerosols, clouds, and radiation processes in the real atmosphere and GCM settings. Dust particles absorb and scatter the incoming sunlight and hence influence the radiation field, referred to as the direct radiative effect. Meanwhile, due to the heating of the air column by dust aerosols, the cloud field can be modified and hence exert cloud radiative forcing, referred to as the semi-direct effect. When aerosols are present in the cloudy atmosphere, another process may take place such that the cloud particle number increases due to the increased loading of aerosols serving as cloud condensation nuclei (CCN) or ice nuclei (IN). Consequently, the cloud particle size decreases and hence affects cloud radiative forcing. This process is known as the first indirect effect since it is through the modification of cloud fields due to changes in CCNs or INs associated with aerosols.

Among all types of aerosols absorbing aerosols, such as dust, play an important role in regional and global climate by heating the air column, which in turn modifies the horizontal and vertical temperature gradient, atmospheric stability, and convection strength (Miller and Tegen, 1998; Menon et al., 2002; Gu et al., 2006). The interactions between dust and other physical processes have been found to play an important role in the dust-induced climate change (Yue et al., 2010). Using a general circulation model (GCM), Miller and Tegen (1998) examined the climatic effect of dust and found that precipitation had been reduced over the tropical North Atlantic and adjacent continental areas including the Sahel region. Further studies show that the surface radiative forcing exerted by dust aerosols also plays an important role in modulating hydrologic cycles (Miller et al., 2004). Gu et al. (2006) investigated the climatic effects of various types of aerosols in China using the atmospheric GCM (AGCM) developed at the University of California, Los Angeles (UCLA) and reported that dust particles in China would heat the air column in the mid- to high latitudes and tend to move the simulated precipitation inland, i.e., toward the Himalayas. Lau et al. (2009) also found that Saharan dust particles during the boreal summer influence rainfall by heating the upper atmosphere above dust layers and drawing in low-level moist air from the Atlantic into the Sahel. The role of direct radiative forcing of dust in the wet-to-dry climate change observed in the Sahel region over the last three decades has been examined by Yoshioka and Mahowald (2007), who showed that precipitation over the inter-tropical convergence zone (ITCZ), including the Sahel region, was reduced, while increased precipitation was found south of the ITCZ, when dust radiative forcing is included in AGCM simulations. They also found that the direct radiative forcing by an increase in North African dust can only explain up to 30% of the observed precipitation reduction in the Sahel.

While the direct radiative forcing of dust aerosols has been studied extensively in recent years, the impact of the overall dust climatic effects, including direct, semi-direct, and indirect forcings, on global and regional climate remains largely unknown (IPCC, 2007). To date, quantification of the first indirect effect of aerosols on climate remains a challenging problem. Inadequate understanding of the relationship between microphysical and dynamical processes contributes to large uncertainties in model simulations of the aerosol effects on clouds, precipitation, and climate, especially for ice clouds, due primarily to the lack of accurate global-scale observations. New data from NASA's A-Train constellation (L'Ecuyer and Jiang, 2011) coupled with recent developments in climate modeling provides an unprecedented opportunity to advance the understanding of aerosol-cloud-radiation interactions and their climatic impact.

The aerosol first indirect effect is associated with change in cloud particle size, a critical and independent parameter that affects radiation transfer calculations. For example, for

a given ice water content (IWC) in clouds, smaller particles reflect more sunlight than larger counterparts, an effect recognized by Twomey et al. (1984) and Liou and Ou (1989) in conjunction with aerosol-cloud indirect effects. Simulation of the aerosol effect on ice particle size in a GCM by means of the physically-based aerosol-ice microphysical interaction would involve large uncertainties in the parameterization of ice processes and require significant computational efforts. A number of formulations have been introduced to relate aerosol concentration to ice nucleation on the basis of explicit microphysics modeling, laboratory studies, as well as theoretical considerations (e.g., Diehl and Mitra, 1998; Kärcher and Lohman, 2003; Riemer et al., 2004; Liu and Penner, 2005; Kärcher et al., 2006; Liu et al., 2007). In view of large uncertainties in the parameterization of ice microphysics processes and the required computational cost, it has been a common practice to prescribe a mean ice crystal size in GCMs (e.g., Köhler, 1999; Ho et al., 1998; Gu et al., 2003). A number of GCMs have also used IWC and temperature produced from the model to determine ice crystal size (Kristjánsson et al., 2005; Gu and Liou, 2006). This approach is rooted in earlier ice microphysics observations from aircraft and attests to the fact that small and large ice crystals are related to cold and warm temperatures in cirrus cloud layers. Ou and Liou (1995) developed a parameterization equation relating cirrus temperature to a mean effective ice crystal size (D_e) based on a large number of midlatitude cirrus microphysics data presented by Heymsfield and Platt (1984). Liou et al. (2008) recently developed a correlation analysis involving IWC and D_e on the basis of fundamental thermodynamic principles intended for application to climate models. For this purpose, ice crystal size distributions obtained from in situ measurements collected during numerous field campaigns in the tropics, midlatitude, and Arctic regions were used. It is shown that IWC and D_e are well-correlated in this regional division. However, none of these formulations take into account the effect of aerosols on D_e ; i.e., the first indirect effect of aerosol on ice clouds.

Combining nearly-simultaneous measurements from Aura Microwave Limb Sounder (MLS) and Aqua Moderate Resolution Imaging Spectroradiometer (MODIS), Jiang et al. (2008) showed substantially different D_e as well as D_e -IWC relations for “polluted” and “clean” clouds over the South American region. Using least-squares fitting to the observed data, an analytical formula to describe the variation in D_e with IWC and AOD for several regions with distinct characteristics of D_e -IWC-AOD relationships has been obtained (Jiang et al., 2011). Because IWC is directly related to convective strength and AOD represents aerosol loading, this empirical formula provides a means of quantifying the relative role of dynamics and aerosols in controlling D_e in different geographical regions, and at the same time of establishing a framework for parameterization of aerosol effects on D_e in climate models. In this study, we have used the D_e -IWC-AOD relations derived from satellite data for

application to GCMs in terms of parameterization of the effective ice particle size in association with the aerosol first indirect effect.

The semi-direct effect was first reported by Hansen et al. (1997) to describe the aerosol absorption of sunlight which heats the lower troposphere and reduces large-scale cloud cover. This effect could be comparable to or even offset the aerosol direct and/or indirect effects (Gu et al., 2006). Studies have shown a great complexity in the cloud response to the heated layer, depending on the relative position of the absorbing aerosol layer with reference to the cloud (Johnson et al., 2004; Fan et al., 2008), the underlying surface (Allen and Sherwood, 2010; Koch and Genio, 2010), etc. At present, the semi-direct effect is poorly understood and its role in the forcing of cloud distributions and regional climate change is intricate and physically unclear (Koch and Del Genio, 2010).

The objective of this study is to investigate the impact of dust aerosols on regional climate with a focus on the North Africa region, by examining the responses of the regional climate system to direct, semi-direct, and first indirect (with a focus on ice clouds) aerosol radiative forcings in the UCLA AGCM in terms of the cloud, radiation, temperature, precipitation, and general circulation patterns. The organization of this paper is as follows: in Sect. 2 we present the model employed and its radiation/cloud parameterizations for aerosols, followed by offline studies on aerosol-radiation-cloud interactions and a description of the AGCM experiment design in Sect. 3. The model simulations and discussions are presented in Sect. 4. Conclusions are given in Sect. 5.

2 Model description and parameterizations for aerosol direct and first indirect effects

For the AGCM simulations, we use a modified version of UCLA AGCM, a state-of-the-art grid point model of the global atmosphere extending from the Earth’s surface to a height of 50 km. This model has been successfully applied to a number of climate studies, including El Niño and the Asian Monsoon (e.g., Arakawa, 1999; Mechoso et al., 1999). In the UCLA AGCM, the geographical distribution of sea surface temperature is prescribed based on a 31-yr (1960–1990) climatology corresponding to the GISST version 2.2 dataset (Rayner et al., 1995). Sea ice thickness and extent are prescribed using data presented by Alexander and Mobley (1976). Surface albedo and roughness length are specified following Dorman and Sellers (1989). Note that the SST response may play an important role in the simulation of the climatic effect of mineral dust aerosols. Based on the study of Yue et al. (2011), the SST responses could influence the simulated dust-induced climate change, especially when climate simulations consider the two-way dust-climate coupling to account for feedbacks. Recently, an improved physically based radiation scheme has been incorporated in

the UCLA AGCM with the capability to study a variety of climate problems, including the cloud and aerosol effects (Gu et al., 2003, 2006, 2011; Gu and Liou, 2006). To assess the performance of GCMs in simulating upper-tropospheric IWC, a new set of IWC measurements from the Earth Observing System's MLS were used to compare with simulations from several GCMs, including the updated UCLA AGCM with the Fu-Liou-Gu radiation scheme. Results showed that the UCLA AGCM is capable of capturing the global distributions of IWC as compared to MLS data and is among the best in terms of simulated IWC values (Li et al., 2005). Although the focus here is the UCLA AGCM, the procedures and parameterizations developed in this research can be readily applied to other climate models. In this study, we have used a low-resolution version with a grid size covering 4° latitude by 5° longitude and with a vertical coordinate of 15 layers from the Earth's surface to 1 hPa. A higher resolution may be better to capture the regional characteristic of clouds. However, since the focus of this study is on the dust climatic effect in the North Africa region, the current model resolution appears to be sufficient for this purpose. In fact, this type of resolution has been used in numerous climate simulations (e.g., Hansen et al. 2004; Köhler, 1999).

The Fu-Liou-Gu radiation scheme (Gu et al., 2010, 2011) implemented in the UCLA AGCM was based on the Fu-Liou scheme. Fu et al. (1997) showed that the delta-two-stream method is most computationally efficient but produces significant errors in fluxes and heating rates under cloudy conditions. High accuracy can be obtained by using the delta-four-stream method, but substantial computer time is required for the calculation of thermal infrared (IR) radiative transfer. The delta-two/four-stream combination method is sufficiently economical for IR calculations (four times faster than delta-four-stream, but only 50 % slower than two-stream), and at the same time it produces acceptable accuracy under most atmospheric conditions. In view of the above, we implement in the UCLA AGCM a combination of the delta-four-stream approximation for solar flux calculations (Liou et al., 1988) and delta-two/four-stream approximation for IR flux calculations (Fu et al., 1997).

The incorporation of nongray gaseous absorption in multiple-scattering atmospheres is based on the correlated k -distribution method developed by Fu and Liou (1992), in which the cumulative probability of the absorption coefficient, g , in a spectral interval is used as an independent variable to replace the wavenumber. The solar and IR spectra are divided into 6 and 12 bands, respectively, according to the location of absorption bands. Using the correlated k -distribution method, 121 spectral radiation calculations are required for each vertical profile in the AGCM. In addition to the principal absorbing gases listed in Fu and Liou (1993) and Gu et al. (2003), we recently included absorption by water vapor continuum and a number of minor absorbers in the solar spectrum, including CH_4 , N_2O , NO_2 , O_3 , CO , SO_2 , $\text{O}_2\text{-O}_2$, and $\text{N}_2\text{-O}_2$. This led to an additional absorption of

solar flux in a clear atmosphere on the order of $1\text{--}3\text{ W m}^{-2}$ depending on the solar zenith angle and the amount of water vapor employed in the calculations (Zhang et al., 2005).

In conjunction with the radiation parameterization, we have also developed a new cloud formation scheme. We define the fractional cloudiness (C_f) by linear interpolation in $\log_{10}q_t$ between $q_t = 10^{-10}\text{ kg kg}^{-1}$ corresponding to the upper limit of cloud free condition ($C_f = 0$) and $q_t = 10^{-5}\text{ kg kg}^{-1}$ corresponding to overcast condition ($C_f = 1$), where q_t is the predicted water content. Producing partial cloudiness introduces the cloud vertical overlap problem, which is an important issue in climate model studies. Various parameterizations of the cloud overlap effect have been developed, and several AGCM-sensitivity tests have been performed (e.g., Liang and Wang, 1997; Chou et al., 1998; Gu and Liou, 2001). The most common methods used in the contemporary AGCMs are random overlap (Manabe and Strickler, 1964) and maximum/random overlap (Geleyn and Hollingsworth, 1979; Chou et al., 1998). The latter has been shown to be more consistent with the observed cloud distribution (Tian and Curry, 1989). Here we employ the method of maximum/random overlap, in which clouds are divided into three types according to their heights: low, middle, and high. Maximum overlap is used for clouds of the same type, while random overlap is subsequently employed for clouds of different types. Scaling of the optical depth in groups of clouds of the same type is performed in terms of cloud cover based on the method introduced by Chou et al. (1998). An atmospheric column, therefore, can be divided into at most 8 sectors if clouds are present in all of the three groups. Radiation calculations can then be performed for each of the cloud configurations and the all-sky flux can be determined as the weighted sum of the flux computed for each sector.

2.1 Parameterization of the aerosol direct effect

The radiative properties of atmospheric aerosols, including the extinction coefficient, single-scattering albedo, and asymmetry factor, must be determined from their composition, shape, and size distribution. Many commonly used GCMs to date either neglect the atmospheric aerosol effect or simply use average values for the optical properties in the calculations. For example, Menon et al. (2002) used a single-scattering albedo value of 0.85 involving an aerosol composition of 85 % sulfate and 15 % black carbon, and a value of 1 for pure sulfate, for all wavelengths. Some models concentrate on specific aerosol types, such as volcanic aerosols, desert aerosols, or aerosols produced by biomass burning. Aerosols in the atmosphere are assumed to be a mixture of different components, referred to as aerosol types. In the new radiation scheme for the UCLA AGCM, a total of eighteen aerosol types are parameterized by using the recent addition of the Optical Properties of Aerosols and Clouds (OPAC) database (d'Almeida et al., 1991; Tegen and Lacis, 1996; Hess et al., 1998). These aerosol types include

maritime, continental, urban, five different sizes of mineral dust, insoluble, water soluble, soot (black carbon), sea salt in two modes (accumulation mode and coarse mode), mineral dust in four different modes (nucleation mode, accumulation mode, coarse mode, and transported mode), and sulfate droplets. The database provides the single-scattering properties for spherical aerosols computed from the Lorenz-Mie theory in which the humidity effects are accounted for. For aerosols that are able to take up water, the single-scattering properties for eight sets of humidity are provided in OPAC database: 0%, 50%, 70%, 80%, 90%, 95%, 98%, and 99%. For each model grid point, the single-scattering properties of dust particles are interpolated based on the model simulated humidity using the eight datasets. The lognormal distribution function was used which was found to be suitable to characterize the size distribution of atmospheric aerosols (d'Almeida et al., 1991; Hess et al., 1998).

In our current radiation scheme for the UCLA AGCM, the single-scattering properties for the 18 aerosol types for 60 wavelengths in the spectral region between 0.3 μm and 40 μm are interpolated into the Fu-Liou spectral bands. These properties are vertically distributed and dependent on the aerosol type and relative humidity. As an example, Fig. 2 shows the single-scattering albedo, extinction coefficient, and asymmetry factor as a function of wavelength for sulfate, dust, and soot, respectively. It can be seen that sulfate mostly scatters solar radiation with a single-scattering albedo close to 1.00 for the first few solar bands. Black carbon (or soot) with a single-scattering albedo of about 0.2 or less in the visible, on the other hand, absorbs substantial solar radiation. Larger dust particles have an averaged single-scattering albedo of about 0.7 (in the visible) and produce both scattering and significant absorption of solar radiation. These results also show that dust may have a significant effect on IR radiative forcing.

2.2 Parameterization of aerosol first indirect effect on ice cloud

The aerosol first indirect effect is related to the radiative forcing caused in the change of cloud particle size and hence the modification of the single-scattering properties of a cloud due to the presence of larger aerosol loadings. For the aerosol effect on D_e , we follow the approach presented by Jiang et al. (2011), in which an analytical formula was obtained to describe the variations of D_e with IWC and AOD for several regions with distinct characteristics of D_e -IWC-AOD. Using MLS IWC measurements at 215 hPa to indicate convective strength (CONV) and AOD measurements from MODIS to denote aerosol loading, as well as using a least-squares fitting, an empirical formula for ice cloud effective radius r_e ($D_e/2$) as a function of CONV and AOD was derived to approximately capture the observed relationships among these three parameters as follows:

$$r_e = \varepsilon \cdot \text{AOD}^\eta \cdot [1 - \exp(-\text{CONV}/\alpha)] \cdot \exp(-\beta \cdot \text{CONV}), \quad (1)$$

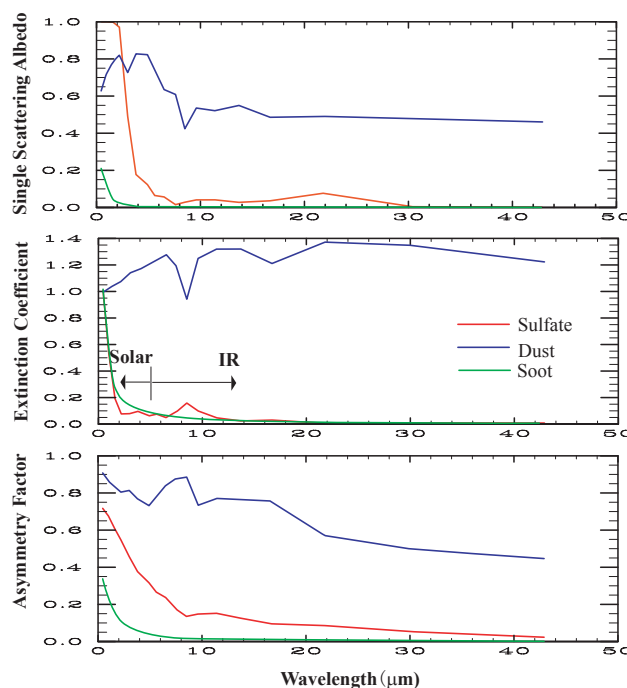


Fig. 2. Single scattering albedo (top panel), extinction coefficient (middle panel), and asymmetry factor (bottom panel) as a function of wavelength for sulfate (red), dust (blue), and soot (green).

where ε , α , β , and η are coefficients determined by performing a two-dimensional least-squares fitting to the observed data. CONV is the convective index defined in terms of IWC as $\text{CONV} = \text{IWC}/\overline{\text{IWC}}$, where IWC represents an individual measurement and $\overline{\text{IWC}}$ is the mean of all measurements. The results of the fitted parameters for the global area, LON: 0°–360°; LAT: 50° S–50° N, and the five different regions are given in Jiang et al. (2011). The choice of these five regions was based on the previous study reported in Jiang et al. (2009), where ice cloud particle sizes in these regions were shown to correlate well with aerosol loadings. These regions are: South America (LON: 270°–340°; LAT: 40° S–10° N); Southern Africa (LON: 0°–55°; LAT: 35° S–0°); Northern Africa (LON: –10°–45°; LAT: 0° S–25° N); South Asia (LON: 70°–120°; LAT: 10° S–15° N); and East Asia (LON: 90°–180°; LAT: 20°–45° N). In this study, the relationship derived for the North Africa region was used, in which $\varepsilon = 23.703$, $\alpha = 0.259$, $\beta = 0.00678$, and $\eta = -0.0589$. Note that this D_e -IWC-AOD relation only works for AOD larger than 0. When there is no aerosol, D_e must be prescribed or calculated from other cloud microphysical parameterizations. In this study, a prescribed D_e with a value of 85 μm based on available ice crystal sizes determined from six observational campaigns reported by Fu (1996) was used in the clean conditions of off-line studies. Note that the D_e -IWC-AOD relationships (Jiang et al., 2011) have been

derived from the climatological satellite data and are the same throughout the year. Their seasonal variation and its impact on climate simulations will require further analysis. Also these relationships were derived by using the IWC at 215 hPa, because ~ 200 hPa is approximately the level of convective detrainment and the IWC is proportional to convective intensity. In order to parameterize D_e in a vertically inhomogeneous atmosphere, substantial research is needed and will be a subject of further investigation.

For inclusion of the aerosol indirect effect in a GCM to investigate the radiative forcing caused by the change of ice crystal size induced by the presence of aerosols, we follow the procedure developed by Fu and Liou (1993) for parameterization of the single-scattering properties of ice particles with their sizes modified by aerosols. Calculations of the single-scattering properties for clouds require information about the particle shape and size distributions, as well as the indices of refraction as a function of wavelength. The spectral extinction coefficient, the single-scattering albedo, and the asymmetry factor are parameterized in terms of ice/liquid water content and mean effective particle size.

Input to the Fu-Liou-Gu radiative transfer program includes the optical depth τ , the single-scattering co-albedo ϖ_0 , and the polynomial coefficients ϖ_i for phase function expansion in the context of the delta-four-stream approximation for radiative transfer, which are, respectively, given by

$$\tau = \text{IWP}(a_0 + a_1/D_e + a_2/D_e^2), \quad (2)$$

$$1 - \varpi_0 = b_0 + b_1 D_e + b_2 D_e^2, \quad (3)$$

$$\varpi_i = c_{0i} + c_{1i} D_e + c_{2i} D_e^2, i = 1 - 4, \quad (4)$$

where IWP (ice water path) is the product of IWC and cloud thickness. The asymmetry factor $g = \varpi_1/3$ and a_n , b_n , and c_{ni} ($n=0, 1, 2$; $i=1-4$) are fitting coefficients determined from the basic scattering and absorption database provided in Yang et al. (2000) for solar spectrum and Yang et al. (2005) for thermal infrared spectrum, in which a cirrus cloud is assumed to have mixed habits. For midlatitude, the habit information is derived from the First ISCCP Regional Experiment (FIRE) I and II data, with 50 % bullet rosettes, 25 % plates, and 25 % hollow columns for $L < 70 \mu\text{m}$ and 30 % aggregates, 30 % bullet rosettes, 20 % plates, and 20 % hollow columns for $L > 70 \mu\text{m}$. For tropical cirrus clouds, 33.7 % columns, 24.7 % bullet rosettes, and 41.6 % aggregates are assumed based on the Central Equatorial Pacific Experiment (CEPEX) data (McFarquhar, 2001).

For solar bands, the first-order polynomial expansion is sufficient to achieve 0.1 % accuracy. However, for thermal infrared bands, the second-order polynomial fitting is required to achieve this level of accuracy. Figure 3 illustrates the single-scattering albedo, extinction coefficient, and asymmetry factor as a function of wavelength for different

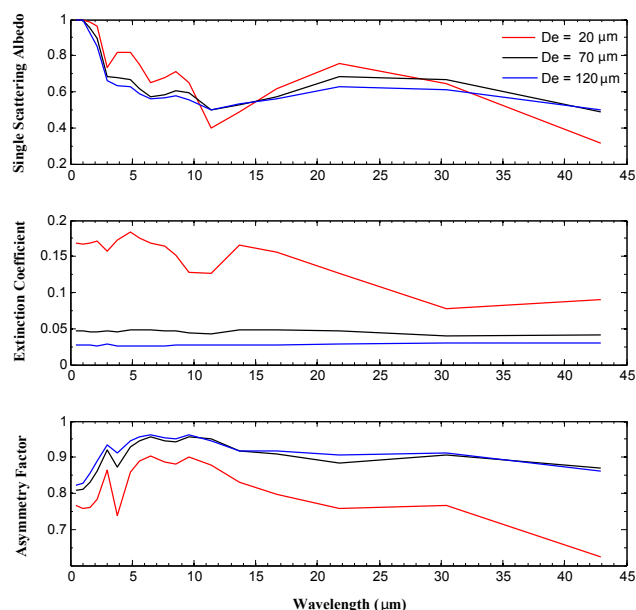


Fig. 3. Single scattering albedo (top panel), extinction coefficient (middle panel), and asymmetry factor (bottom panel) as a function of wavelength for different ice crystal mean effective sizes calculated based on mixed habits.

ice crystal effective sizes under the mixed habit assumption (Yue et al., 2007). It is shown that smaller ice crystal size generally corresponds to larger single-scattering albedo, larger extinction coefficient, and smaller asymmetry factor, which will lead to more reflected solar fluxes as well as more trapped IR fluxes in radiative transfer calculations.

The effective radius for water clouds is fixed at $10 \mu\text{m}$ in this study. For ice clouds, the ice crystal effective size is parameterized using the model predicted IWC and the D_e -IWC-AOD relations obtained from the A-Train satellite data for North Africa region, as previously discussed.

3 Offline studies

Prior to the AGCM simulations, we examined the off-line one-column radiative effects of dust aerosols, including direct, indirect, as well as semi-direct, using the Fu-Liou-Gu radiative transfer model. In order to examine the aerosol semi-direct effect associated with the aerosol absorption of sunlight, which leads to the heating of the atmosphere and reduces large-scale cloud covers (Hansen et al., 1997), we have used larger absorptive dust particles in this study. For smaller dust particles which scatter solar radiation, smaller absorption would be produced in the atmosphere, leading to a negative radiative forcing at TOA (Gu et al., 2006). The atmospheric profile used represents the standard atmosphere condition. The input aerosol optical depth represents the vertically integrated column values, which have been distributed

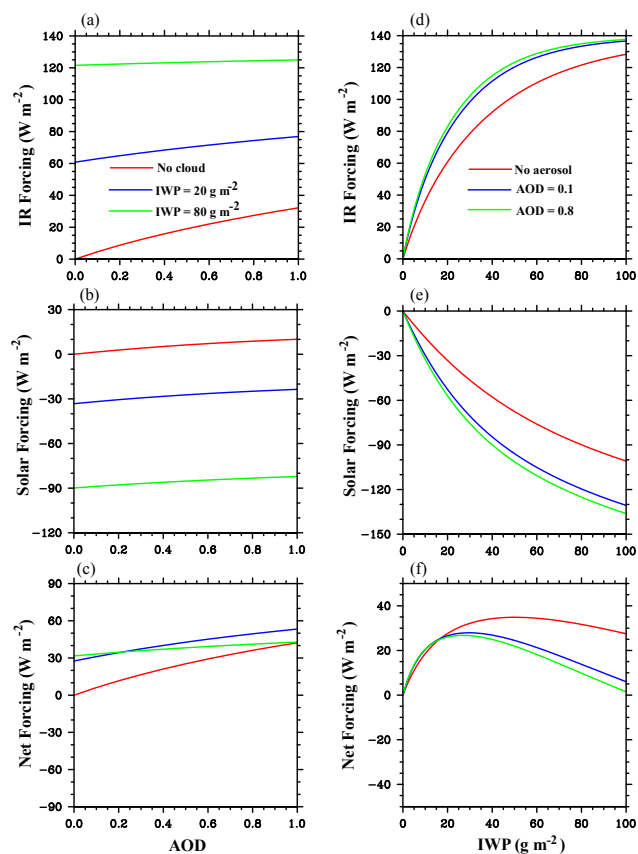


Fig. 4. Aerosol and cloud IR (a, d), solar (b, e), and net (c, f) forcings (W m^{-2}) at TOA as a function of AOD (left panel) and IWP (right panel), respectively.

vertically according to a certain weighting profile based on the layer pressure and scale height, a height at which the aerosol loading is reduced to e^{-1} of the surface value, which is set at 3 km in this study. The aerosol loading decreases exponentially such that the highest aerosol layer in the model is placed at 15 km (Charlock et al., 2004). Consequently, the spectral single-scattering properties are dependent on height according to aerosol type and relative humidity. The aerosols were assumed to be spherical in shape, an assumption that is not applicable to dust and black carbon and is a subject requiring further study. In order to identify the aerosol direct, first indirect and semi-direct effects, both clear and cloudy conditions were assumed in various experiments. The cosine of the solar zenith angle of 0.5 and a surface albedo of 0.1 were used in the calculations. For aerosol indirect effect, the D_e -IWC-AOD relationship derived for the North Africa region was used. For cloudy conditions, the ice cloud layer for the offline study is placed between 9 and 11 km.

Figure 4a–c shows the IR, Solar, and net radiative forcings at the top of the atmosphere (TOA) as a function of dust AOD, ranging from 0–1.0, for clear and cloudy conditions. For cloudy conditions, we show two cases with

IWP of 20 g m^{-2} and 80 g m^{-2} , with corresponding cloud optical depths of 0.75 and 3.0, respectively. The forcing for clear condition represents the aerosol direct effect, while semi-direct effect can be inferred from the results for cloudy conditions. Direct solar radiative forcing for dust aerosol is positive at TOA due to its absorption. The solar, IR, and net forcings generally increase with increasing AOD, with a net of 25 W m^{-2} for AOD=0.5 and 40 W m^{-2} for AOD=1. Note that the positive IR forcing for dust aerosols contributes to about 75% of the net forcing. Quijano et al. (2000) have estimated the instantaneous TOA dust radiative forcing over desert for AOD=1.0 to be in the range of 50 – 55 W m^{-2} , which agrees rather well with the values reported in this study. At the surface, a negative net forcing of about -40 W m^{-2} is found for AOD=0.5 due to the scattering and absorption by dust particles (not shown). Kim et al. (2010) reported a negative forcing by dust at the surface with a value of about -55 W m^{-2} around local noontime. Using the Goddard Institute for Space Studies GCM, Liao and Seinfeld (2004) also pointed out that the surface cooling could reach values as high as -30 W m^{-2} , mainly caused by the absorptive aerosols such as mineral dust and black carbon. The radiative forcing estimated from current study agrees well with their results. When ice clouds are present simultaneously with the dust aerosols, positive IR radiative forcing is enhanced since ice clouds trap substantial IR radiation, while the positive solar forcing with dust aerosols alone has been changed to negative values due to the strong reflection of solar radiation by clouds, indicating that cloud forcing could exceed aerosol forcing. Overall, IR forcing is still stronger than negative solar forcing in cloudy cases, resulting in a net positive forcing for aerosol-cloud cases at TOA. With the presence of ice clouds, the solar, IR, and net forcings still increase with increasing AOD but with a much smaller slope. As a result, when AOD is approaching 1.0, the net forcing with the combined aerosol and cloud effects is approximately equivalent to that with dust aerosol alone. This means that under heavily dusty cases, the cloud radiative forcing can be masked by the dust direct radiative forcing. In a GCM setting, aerosol absorption of sunlight can heat the lower troposphere and reduce cloud cover and/or cloud ice water content. When aerosol loading is small (AOD < 0.2), the net combined aerosol-cloud forcing is particularly significant for IWP = 80 g m^{-2} . However, the net aerosol-cloud forcing for a smaller IWP becomes substantial and increases with AOD for AOD > 0.2, indicating that the aerosol effect modulates cloud forcing. The aerosol semi-direct effect could exert an extra net forcing of about 10 W m^{-2} for heavily polluted case with AOD = 1.0 along with the reduction in cloud IWP from 80 g m^{-2} to 20 g m^{-2} .

Figure 4d–f illustrates the IR, Solar, and net radiative forcings at the TOA as a function of IWP, ranging from 0– 100 g m^{-2} , with cloud optical depth ranging from 0–3.75, for clean and polluted (aerosol indirect effect) cloudy cases. For polluted cases, results for AOD values of 0.1 and 0.8

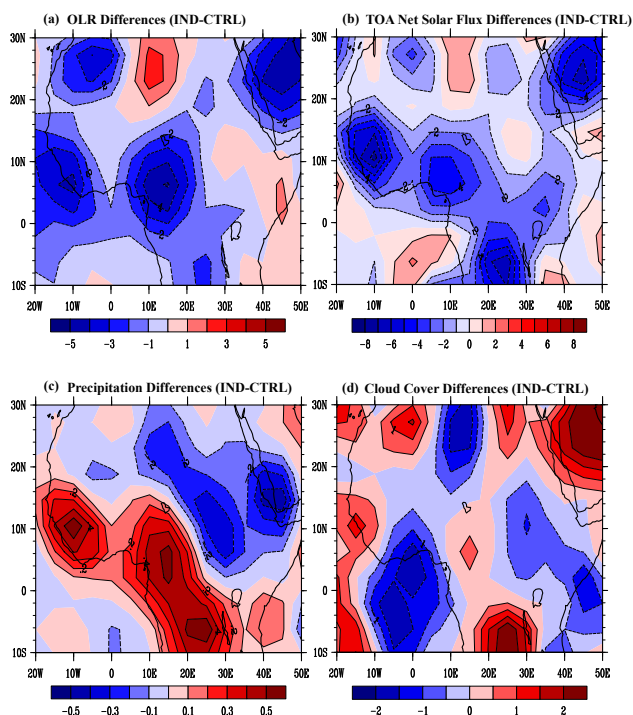


Fig. 5. JJA differences in (a) OLR (W m^{-2}), (b) TOA net solar flux (W m^{-2}), (c) precipitation (mm day^{-1}), and (d) cloud cover (%) between experiments IND and CTRL.

are shown in the figure. Under clean cloud condition, the magnitudes of positive IR forcing and negative solar forcing increase with increased IWP, with values comparable to those from Fu and Liou (1993). For polluted cases, higher AOD corresponds to smaller ice crystals, resulting in more trapped IR and larger reflected solar radiation. With the aerosol indirect effect, the net cloud forcing is reduced for $\text{IWP} > 20 \text{ g m}^{-2}$. The magnitude of reduction increases with IWP, with a decrease of about 25 W m^{-2} in the net TOA forcing for $\text{IWP} = 100 \text{ g m}^{-2}$ and $\text{AOD} = 0.8$.

4 AGCM simulations

In the real atmosphere, aerosol direct and indirect effects take place simultaneously. Aerosol indirect effect can be masked by its direct radiative forcing when the latter is included. Therefore, it is our intent to examine the aerosol indirect effect with and without the presence of aerosol direct radiative forcing. In accordance with our research objective, we have performed a series of experiments using the updated UCLA AGCM described above. Each simulation is a 5-yr run with the initial condition corresponding to 1 October (climatologically). The effect of greenhouse gases and other forcings are fixed in all experiments so that aerosols are the only varying forcing between the experiments in this study. A summary

of the model experiments are described below and shown in Table 1.

1. CTRL: in the first set of the experiment, the D_e -IWC-AOD relationship for “clean” clouds is used everywhere with a background AOD of 0.1. Aerosol direct radiative forcing is not included in this experiment. This experiment is considered as the control run, which represents the case without aerosol effect.
2. IND: the second set of the experiment is identical to (1), except that the D_e -IWC-AOD relation for “polluted” clouds is used for North Africa with $\text{AOD} = 0.5$ to include the aerosol indirect effect while AOD of 0.1 is used elsewhere. The selection of this AOD value is based on the observed climatological value of AOD for the North Africa region (Satheesh et al., 2006).
3. DIR_IND: the last experiment examines the total effect of aerosol direct and indirect radiative forcings. This experiment is identical to (2) but includes both aerosol indirect and direct effects for the North Africa area. Dust particle is used as the aerosol type in the simulation for the aerosol direct effect.

Differences between experiments (1) and (2) show the sensitivity of aerosol first indirect radiative forcing due to the dust aerosols in North Africa. Comparisons between experiments (2) and (3) demonstrate the relative importance of aerosol direct as well as semi-direct or indirect effects when its counterpart is also included. Differences between (1) and (3) illustrate the overall aerosol effects. Interactions between aerosols and cloud/radiation fields and their influence on the atmosphere thermal structure and dynamic processes through the modification of the heating rate profile are examined in the next section.

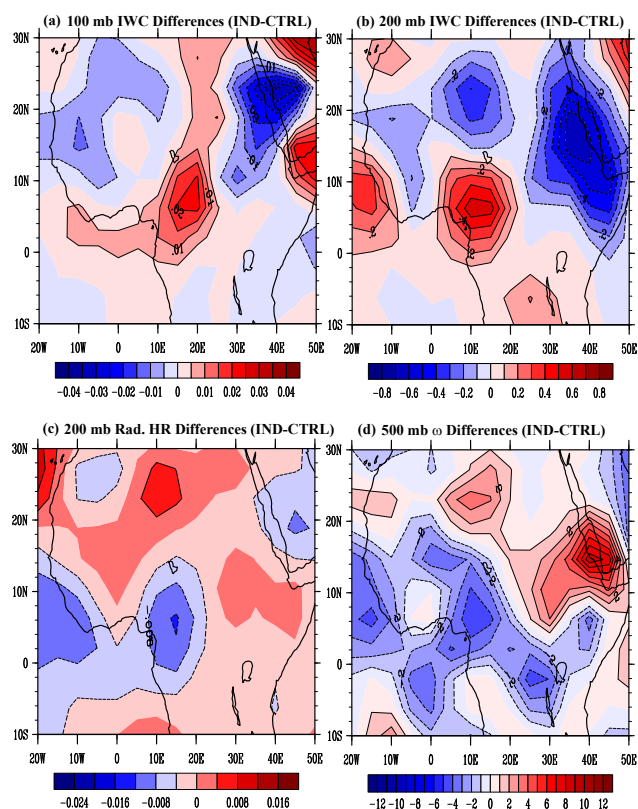
We first evaluate the indirect radiative effect of aerosols by comparing the 5-yr simulation results of the experiments IND and CTRL. We have also extended climate simulations to 20 yr. Differences between the last 5-yr mean simulation results and the control run have similar patterns as those presented in the first 5-yr means. For this reason, results are presented in terms of the first 5-yr means. During the boreal summer, June–July–August (JJA), the rainfall system in West Africa could be significantly affected by dust particles. Also, since differences between the sensitivity experiments and the control run are mainly located in the summer hemisphere associated with the position of the sun, results are presented in terms of the JJA means. Figure 5a–b shows the JJA differences in OLR and net solar flux at TOA for the North Africa region due to the aerosol indirect effect. Due to the smaller ice crystal size in the dusty case, OLR is reduced over the mostly cloudy North Africa region partly because ice clouds with smaller size trap more IR radiation. The net solar flux at TOA is also reduced because smaller sizes reflect more solar radiation. The net radiative forcing at TOA, including both

Table 1. Experiment design using D_e -IWC-AOD relationship derived for North Africa region.

Experiment	Direct effect	Indirect effect	AOD
Control: clean (CTRL)	None	None	AOD = 0.1 NOTE: this control run represents the case without aerosol effect
Indirect: polluted (IND)	None	Yes	AOD = 0.5 for North Africa AOD = 0.1 elsewhere
Direct and Indirect (DIR_IND)	Yes Aerosol Type: dust	Yes (North Africa)	AOD = 0.5 for North Africa AOD = 0.1 elsewhere

solar and IR, shows negative in the North Africa region. This is in line with the offline calculation result which illustrates the reduction in net forcing when aerosol indirect effect is included (Fig. 4f). Precipitation in the same area, however, increases due to aerosol indirect effect on ice clouds (Fig. 5c), corresponding to the enhanced convection as indicated by reduced OLR, while the cloud cover shows decreases between 10°S – 10°N across North Africa and the Atlantic with an increase to the west (Fig. 5d). Differences between the sensitivity experiment IND and CTRL are statistically significant at the confidence level typically exceeds 95 % corresponding to the major changes in the OLR, precipitation, and cloud cover fields in North Africa. Anomalies are shown to be significant in all areas at above 70 % level. Note that the aerosol 2nd indirect effect, which is on the precipitation rate, is not included. Change in precipitation is through the interactions among aerosol, cloud, radiation, and dynamical processes in the model. Mahowald and Kiehl (2003) found a negative correlation between high cloud amount and dust along the equator across North Africa and the Atlantic in a region of relatively large ice cloud amount. They also indicated that there was a positive anomalies to the west, indicating a shift in the location of ice clouds although there might be a net increase in ice cloud cover. Our simulation results appear to be in line with this observation. However, they also indicated that since there are no long-term ground measurements for dust and high clouds in these areas, and because it has been difficult to map these high clouds using satellite observations, making a firm conclusion regarding high clouds, precipitation, and ice forming around dust kernels is not a straightforward task. Further in-depth studies are needed from both observational and modeling approaches.

Figure 6a–b depicts the differences in IWC at 100 and 200 mb, respectively. Corresponding to increased precipitation, we show that IWCs are increased in this region. The differences in liquid water content show the same patterns as in IWC but with a much smaller magnitude (not shown), which is expected and appears to be reasonable. In this case, the feedback in water clouds could only slightly contribute to the magnitude of the changes but would not affect the results and conclusions presented in this study. The 200 mb

**Fig. 6.** JJA differences in (a) 100 mb and (b) 200 mb IWC (mg m^{-3}), (c) 200 mb radiative heating rate (K day^{-1}), and (d) 500 mb ω (mb day^{-1}) between experiments IND and CTRL.

radiative heating rate shows more cooling with the aerosol indirect effect (Fig. 6c) in association with the production of larger cooling at the cloud top consisting of smaller ice crystal size. The 500 mb omega indicates a strong upward motion in this region (Fig. 6d), which, together with the increased cooling effect, resulted in the increased ice water contents as shown in Fig. 6a–b.

Figure 7a shows the differences between the simulation with overall aerosol effect (direct + semi-direct + indirect) and that with only the indirect effect. Adding the aerosol

direct effect in the model simulation reduces the precipitation in the normal rainfall band over North Africa, where precipitation is shifted to the south and the northeast, associated with the absorption of sunlight and the subsequent heating of the air column by dust particles. As a result, the rainfall is drawn further inland to the northeast. The increase in precipitation between the equator and 10 degrees latitude is associated with increased convection in that region due to the heating of the air column by dust particles, as well as the aerosol indirect effect which produces more cooling at the cloud top. Using a GCM, Miller and Tegen (1998) found that precipitation had been reduced over the tropical North Atlantic and adjacent continental areas including the Sahel region associated with the direct climatic effect of dust. Yoshioka and Mahowald (2007) also reported that when dust direct radiative forcing was included in AGCM simulations, precipitation over the ITCZ, including the Sahel region, was reduced, while increased precipitation was found south of the ITCZ. Our simulation results are in line with their finding. Changes in cloud cover (Fig. 7b) and OLR (Fig. 7c) show a similar pattern to that of precipitation in association with the change in convection strength. The differences in OLR follow the patterns in cloud cover and precipitation instead of the dust loadings, indicating that the aerosol semi-direct effect plays a critical role in the dust-induced climate change. A decrease in OLR and the consequence of an increase in net radiative forcing is shown, which is also reinforced from offline simulations with the aerosol semi-direct effect (Fig. 4c). Confidence level for the significance of differences between the sensitivity experiments DIR_IND and IND typically exceeds 95 % in association with major changes in the OLR, precipitation, and cloud cover fields in North Africa. The differences between the simulation DIR_IND (with overall aerosol effect) and the CTRL (no aerosol effect) are similar to those between DIR_IND and IND (results not shown), indicating that the direct and semi-direct effects play a dominant role in the overall climatic effect of dust aerosols over North Africa.

5 Conclusions

Climate simulations using an updated version of the UCLA AGCM that incorporates a state-of-the-art aerosol/cloud radiation scheme have been carried out to investigate the relative importance and overall impact of dust direct, semi-direct, and first indirect effects on the cloud field, radiation budget, and precipitation patterns in North Africa. In these regions, we have used the aerosol optical depths of 0.5 based on observed climatological values. Parameterization of the aerosol indirect effect for the North Africa region derived from cloud and aerosol data retrieved from A-Train satellite observations has been employed in these climate model simulations. Key results of our study are summarized in the following.

First, dust direct radiative forcing generally increases with increased AOD. When ice clouds are present, the aerosol

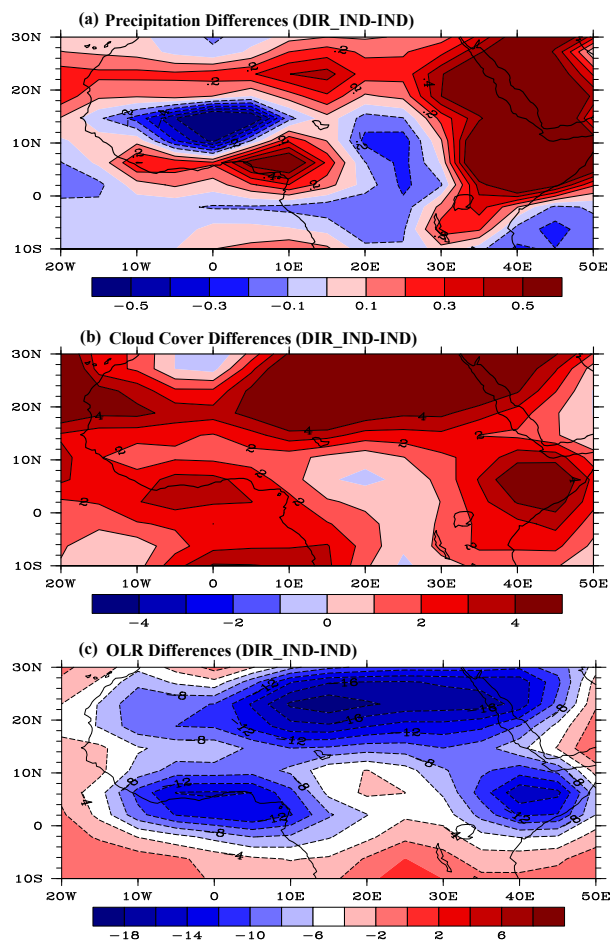


Fig. 7. JJA differences in (a) precipitation (mm day^{-1}), (b) cloud cover (%), and (c) OLR (W m^{-2}) between experiments DIR_IND and IND.

semi-direct effect plays an important role. Positive IR radiative forcing is strengthened with the presence of clouds, while the positive solar forcing with dust aerosols alone has been changed to negative values due to the strong reflection of solar radiation by clouds. Under heavily dusty cases, cloud radiative forcing can be overshadowed by dust direct radiative forcing. In a GCM setting, aerosol absorption of sunlight heats the lower troposphere and reduces cloud cover and cloud ice water amount. The aerosol semi-direct effect could exert an extra net forcing of about 10 W m^{-2} for heavily polluted cases associated with the reduction of cloud ice water amount from 80 g m^{-2} to 20 g m^{-2} . Including the aerosol indirect effect, the net cloud forcing is normally reduced and the magnitude of reduction increases with IWP, with a decrease of about 25 W m^{-2} in net TOA forcing for $\text{IWP} = 100 \text{ g m}^{-2}$ and $\text{AOD} = 0.8$.

Secondly, GCM simulations showed that the reduced ice crystal mean effective size due to the aerosol first indirect effect resulted in less OLR and net solar flux at TOA over the mostly cloudy North Africa region because ice clouds with

smaller size trap more IR radiation as well as reflect more solar radiation. The precipitation in the same area, however, increases due to the action of the aerosol indirect effect on ice clouds, leading to enhanced convection as indicated by reduced OLR. The increased precipitation appears to be associated with enhanced IWCs in this region. The 200 mb radiative heating rate shows more cooling with the aerosol indirect effect since larger cooling is produced at the cloud top, which consists of smaller ice crystal sizes. The 500 mb omega indicates stronger upward motion, which, together with the increased cooling effect at the cloud top, results in increased IWCs.

Finally, including the dust direct and semi-direct effect together with the indirect effect in the model simulation illustrates reduced precipitation in the normal rainfall band over North Africa, where precipitation is shifted to the south and the northeast. Changes in precipitation, cloud cover, and OLR patterns due to the overall effect of dust aerosols is similar to those due to the aerosol direct and semi-direct effects, indicating that aerosol radiative forcing produced by these two effects could be more important than the aerosol first indirect effect in the context of North Africa regional climate.

In the present study, the aerosol second indirect effect on precipitation is not accounted for. The differences in precipitation distribution patterns, therefore, are associated with the interactions and feedback among aerosol, radiation, cloud, and dynamic fields which are modulated by the direct, semi-direct, and first indirect aerosol radiative forcings and in turn affect the simulated climate. Incorporation of the aerosol second indirect effect in the UCLA AGCM is a task we plan to accomplish in future endeavors.

Acknowledgements. This research has been supported by NSF Grants ATM-0924876 and AGS-0946315, DOE Grant DE-SC0006742, NASA ACP program, NASA Aura Science Team, and the Pacific Northwest National Laboratory operated for DOE by Battelle Memorial Institute under contract DE-AC06-76RLO 1830. J. H. Jiang and H. Su acknowledge support by the Jet Propulsion Laboratory, California Institute of Technology, sponsored by NASA.

Edited by: Q. Fu

References

Alexander, R. C. and Mobley, R. L.: Monthly average sea-surface temperatures and ice pack limits on a global grid, *Mon. Weather Rev.*, 104, 143–148, 1976.

Arakawa, A.: A personal perspective on the early years of general circulation modeling at UCLA. General circulation model development: Past, present, and future, Proceedings of a symposium in honor of Professor Akio Arakawa, 20–22 January, 1998, University of California, Los Angeles, edited by: Randall, D. A., Academic Press, 1–65, 2000.

Allen, R. J. and Sherwood, S.: Aerosol-cloud semi-direct effect and land-sea temperature contrast in a GCM, *Geophys. Res. Lett.*, 37, L07702, doi:10.1029/2010GL042759, 2010

Andreae, M. O.: Climatic effects of changing atmospheric aerosol levels, in: *World Survey of Climatology, Volume 16, Future Climates of the World*, edited by: Henderson-Sellers, A., 341–392 (New York: Elsevier), 1995.

Charlock, T. P., Rose, F. G., Rutan, D., Jin, Z., Fillmore, D., and Collins, W.: Global retrieval of the surface and atmospheric radiation budget and direct aerosol forcing, paper presented at Conference on Satellite Meteorology, p. 8.11, Am. Meteorol. Soc., Norfolk, VA, 2004.

Chou, M. D., Suarez, M. J., Ho, C. H., Yan, M. M.-H., and Lee, K.-T.: Parameterizations for cloud overlapping and shortwave single-scattering properties for use in general circulation and cloud ensemble models, *J. Climate*, 11, 202–214, 1998.

Clark, D. B., Xue, Y., Harding, R. J., and Valdes, P. J.: Modeling the impact of land surface degradation on the climate of tropical North Africa, *J. Climate*, 14, 1809–1822, 2001.

d’Almeida, G. A., Koepke, P., and Shettle, E. P.: *Atmospheric aerosols – global climatology and radiative characteristics*, A. Deepak Publishing, Hampton, Virginia, 561 pp., 1991.

Diehl, K. and Mitra, S.: A laboratory study of the effects of a kerosene-burner exhaust on ice nucleation and the evaporation rate of ice crystals, *Atmos. Environm.*, 32, 3145–3151, 1998.

Dorman, J. L. and Sellers, P. J.: A global climatology of albedo, roughness length and stomatal resistance for atmospheric general circulation models as represented by the Simple Biosphere model (SiB), *J. Appl. Meteor.*, 28, 833–855, 1989.

Engelstaedter, S., Tegen, I., and Washington, R.: North African dust emission and transport, *Earth-Science Reviews*, 79, 73–100, 2006.

Fan, J., Zhang, R., Tao, W.-K., and Mohr, K.: Effects of aerosol optical properties on deep convective clouds and radiative forcing, *J. Geophys. Res.*, 113, D08209, doi:10.1029/2007JD009257, 2008.

Fu, Q.: An accurate parameterization of the solar radiative properties of cirrus clouds for climate models, *J. Climate*, 9, 2058–2082, 1996.

Fu, Q. and Liou, K. N.: On the correlated k-distribution method for radiative transfer in nonhomogeneous atmospheres, *J. Atmos. Sci.*, 49, 2139–2156, 1992.

Fu, Q. and Liou, K. N.: Parameterization of the radiative properties of cirrus clouds, *J. Atmos. Sci.*, 50, 2008–2025, 1993.

Fu, Q., Liou, K. N., Cribb, M. C., Charlock, T. P., and Grossman, A.: Multiple scattering parameterization in thermal infrared radiative transfer, *J. Atmos. Sci.*, 54, 2799–2812, 1997.

Geleyn, J.-F. and Hollingsworth, A.: An economical analytical method for the computation of the interaction between scattering and line absorption of radiation, *Beitr. Phys. Atmos.*, 52, 1–16, 1979.

Gu, Y. and Liou, K. N.: Radiation parameterization for three-dimensional inhomogeneous cirrus clouds: Application to climate models, *J. Climate*, 14, 2443–2457, 2001.

Gu, Y. and Liou, K. N.: Cirrus cloud horizontal and vertical inhomogeneity effects in a GCM, *Meteorol. Atmos. Phys.*, 91, 223–235, 2006.

Gu, Y., Fararra, J., Liou, K. N., and Mechoso, C. R.: Parameterization of cloud-radiation processes in the UCLA general circula-

- tion model, *J. Climate*, 16, 3357–3370, 2003.
- Gu, Y., Liou, K. N., Xue, Y., Mechoso, C. R., Li, W., and Luo, Y.: Climatic effects of different aerosol types in China simulated by the UCLA general circulation model, *J. Geophys. Res.*, 111, D15201, doi:10.1029/2005JD006312, 2006.
- Gu, Y., Liou, K. N., Chen, W., and Liao, H.: Direct climate effect of black carbon in China and its impact on dust storm, *J. Geophys. Res.*, 115, D00K14, doi:10.1029/2009JD013427, 2010.
- Gu, Y., Liou, K. N., Ou, S. C., and Fovell, R.: Cirrus cloud simulations using WRF with improved radiation parameterization and increased vertical resolution, *J. Geophys. Res.*, 116, D06119, doi:10.1029/2010JD014574, 2011.
- Hansen, J. and Nazarenko, L.: Soot climate forcing via snow and ice albedos, *Proc. Natl. Acad. Sci., USA.*, 101, 423–428, 2004.
- Hansen, J., Sato, M., and Ruedy, R.: Radiative forcing and climate response, *J. Geophys. Res.*, 102, 6831–6864, 1997.
- Heymsfield, A. and Platt, M.: A parameterization of the particle size spectrum of ice clouds in terms of the ambient temperature and the ice water content, *J. Atmos. Sci.*, 41, 846–856, 1984.
- Hess, M., Koepke, P., and Schult, I.: Optical properties of aerosols and clouds: The software package OPAC, *B. Am. Meteorol. Soc.*, 79, 831–844, 1998.
- Ho, C.-H., Chou, M.-D., Surez, M., and Lau, K. M.: Effect of ice cloud on GCM climate simulations, *Geophys. Res. Lett.*, 25, 71–74, 1998.
- Hoerling, M., Hurrell, J., Eischeid, J., and Phillips, A.: Detection and attribution of 20th century northern and southern African rainfall change, *J. Climate*, 19, 3989–4008, 2006.
- Intergovernmental Panel on Climate Change (IPCC): The physical basis of climate change, Cambridge University Press, The Edinburgh Building Shaftesbury Road, Cambridge, UK, 431 pp., 2007.
- Jiang, J. H., Su, H., Schoeberl, M., Massie, S. T., Colarco, P., Platnick, S., and Livesey, N. J.: Clean and polluted clouds: Relationships among pollution, ice cloud and precipitation in South America, *Geophys. Res. Lett.*, 35, L14804, doi:10.1029/2008GL034631, 2008.
- Jiang, J. H., Su, H., Zhai, C., Massie, S. T., Schoeberl, M. R., Colarco, P. R., Platnick, S., Gu, Y., and Liou, K. N.: Influence of convection and aerosol pollution on ice cloud particle effective radius, *Atmos. Chem. Phys.*, 11, 457–463, doi:10.5194/acp-11-457-2011, 2011.
- Johnson, B. T., Shine, K., and Forster, P.: The semi-direct aerosol effect: impact of absorbing aerosols on marine stratocumulus, *Q. J. Roy. Meteorol. Soc.*, 2004, 1407–1422, 2004.
- Kärcher, B. and Lohman, U.: A parameterization of cirrus cloud formation: Heterogeneous freezing, *J. Geophys. Res.*, 108, 4402, doi:10.1029/2002JD003220, 2003.
- Kärcher, B., Hendricks, J., and Lohman, U.: Physically based parameterization of cirrus cloud formation for use in global atmospheric models, *J. Geophys. Res.*, 111, D01205, doi:10.1029/2005JD006219, 2006.
- Kim, K. M., Lau, W. K.-M., Sud, Y. C., and Walker, G. K.: Influence of aerosol-radiative forcings on the diurnal and seasonal cycles of rainfall over West Africa and Eastern Atlantic Ocean using GCM simulations, *Clim. Dynam.*, 26, doi:10.1007/s00382-010-0750-1, 2010.
- Kristjánsson, J. E., Iversen, T., Kirkevåg, A., Seland, Ø., and Debernard, J.: Response of the climate system to aerosol direct and indirect forcing: Role of cloud feedbacks, *J. Geophys. Res.*, 110, D24206, doi:10.1029/2005JD006299, 2005.
- Koch, D. and Del Genio, A. D.: Black carbon semi-direct effects on cloud cover: review and synthesis, *Atmos. Chem. Phys.*, 10, 7685–7696, doi:10.5194/acp-10-7685-2010, 2010.
- Köhler, M.: Explicit prediction of ice clouds in general circulation models. Ph.D. dissertation, University of California, Los Angeles, 167 pp., 1999.
- Lamb, P. J. and Pepler, R. A.: Further case studies of tropical Atlantic surface atmospheric and oceanic patterns associated with sub-Saharan drought, *J. Climate*, 5, 476–488, 1992.
- Lau, W. K.-M., Kim, K. M., Sud, Y. C., and Walker, G. K.: A GCM study of the response of the atmospheric water cycle of Western Africa and the Atlantic to Saharan dust radiative forcing, *Geophys. Ann.*, 27, 4023–4037, 2009.
- L’Ecuyer, T. S. and Jiang, J. H.: Touring the atmosphere aboard the A-Train, *Physics Today*, 63, 36–41, 2010.
- Li, J.-L., Waliser, D. E., Jiang, J. H., Wu, D.L., Read, W., Waters, J. W., Tompkins, A., Donner, L. J., Chern, J.-D., Tao, W.-K., Atlas, R., Gu, Y., Liou, K. N., Del Genio, A., Khairoutdinov, M., and Gettelman, A.: Comparisons of EOS MLS cloud ice measurements with ECMWF analyses and GCM simulations: Initial Results, *Geophys. Res. Lett.*, 32, L18710, doi:10.1029/2005GL023788, 2005.
- Liang, X.-Z. and Wang, W.-C.: Cloud overlap effects on general circulation model climate simulations, *J. Geophys. Res.*, 102, 11039–11047, 1997.
- Liao, H. and Seinfeld, J.: Global radiative forcing of coupled tropospheric ozone and aerosols in a unified general circulation model, *J. Geophys. Res.*, 109, D16207, doi:10.1029/2003JD004456, 2004.
- Liou, K. N. and Ou, S.: The role of cloud microphysical processes in climate: An assessment from a one-dimensional perspective, *J. Geophys. Res.*, 94, 8599–8607, 1989.
- Liou, K. N., Fu, Q., and Ackerman, T. P.: A simple formulation of the delta-four-stream approximation for radiative transfer parameterizations, *J. Atmos. Sci.*, 45, 1940–1947, 1988.
- Liou, K. N., Gu, Y., Yue, Q., and MacFarguhar, G.: On the correlation between ice water content and ice crystal size and its application to radiative transfer and general circulation models, *Geophys. Res. Lett.*, 35, L13805, doi:10.1029/2008GL033918, 2008.
- Liu, X. and Penner, J.: Ice nucleation parameterization for global models, *Meteorologische Z.*, 14, 499–514, 2005.
- Liu, X., Penner, J., Ghan, S., and Wang, M.: Inclusion of ice microphysics in the NCAR Community Atmospheric Model version 3 (CAM3), *J. Climate*, 20, 4526–4547, 2007.
- Mahowald, N. and Kiehl, L.: Mineral aerosols and cloud interactions, *Geophys. Res. Lett.*, 30, 1475, doi:10.1029/2002GL016762, 2003.
- Manabe, S. and Strickler, R.: Thermal equilibrium of the atmospheres with a convective adjustment, *J. Atmos. Sci.*, 21, 361–385, 1964.
- McFarquhar, G. M.: Comments on “Parameterization of effective sizes of cirrus-cloud particles and its verification against observations” by Zhian Su and Lawrie Rikus (October B, 1999, 125, 3037–3055), *Q. J. Roy. Meteorol. Soc.*, 127, 261–266, 2001.
- Mechoso, C. R., Yu, J.-Y., and Arakawa, A.: A coupled GCM pilgrimage: From climate catastrophe to ENSO simulations.

- General circulation model development: Past, present, and future, Proceedings of a symposium in honor of Professor Akio Arakawa, 20–22 January, 1998, University of California, Los Angeles, edited by: Randall, D. A., Academic Press, 539–575, 2000.
- Menon, S., Hansen, J., Nazarenko, L., and Luo, Y.: Climate effects of black carbon aerosols in China and India, *Science*, 297, 2250–2253, 2002.
- Miller, R. L. and Tegen, I.: Climate response to soil dust aerosols, *J. Climate*, 11, 3247–3267, 1998.
- Miller, R. L., Tegen, I., and Perlwitz, J.: Surface radiative forcing by soil dust aerosols and the hydrologic cycle, *J. Geophys. Res.*, 109, D04203, doi:10.1029/2003JD004085, 2004.
- Nicholson, S. E.: Land surface processes and Sahel climate, *Rev. Geophys.*, 38, 117–139, 2000.
- Ou, S. and Liou, K. N.: Ice microphysics and climatic temperature perturbations, *Atmos. Res.*, 35, 127–138, 1995.
- Prospero, J. M. and Lamb, P. J.: African droughts and dust transport to the Caribbean: Climate change implications, *Science*, 302, 1024–1027, 2003.
- Quijano, A. L., Sokolik, I. N., and Toon, O. B.: Radiative heating rates and direct radiative forcing by mineral dust in cloudy atmospheric conditions, *J. Geophys. Res.*, 105, 12207–12219, 2000.
- Rayner, N. A., Folland, C. K., Parker, D. E., and Horton, E. B.: A new global sea-ice and sea surface temperature (GISST) data set for 1903–1994 for forcing climate models. Internal Note 69, 14 pp, Hadley Center, Met. Office, Bracknell, UK, 1995.
- Riemer, N., Vogel, H., and Vogel, B.: Soot aging time scales in polluted regions during day and night, *Atmos. Chem. Phys.*, 4, 1885–1893, doi:10.5194/acp-4-1885-2004, 2004.
- Rowell, D. P., Folland, C. K., Maskell, K., and Ward, M. N.: Variability of summer rainfall over tropical North Africa (1906–1992): Observations and modeling, *Q. J. Roy. Meteorol. Soc.*, 121, 669–704, 1995.
- Satheesh, S. K. and Moorthy, K.: Radiative effects of natural aerosols: A review, *Atmos. Environm.*, 39, 2089–2110, 2005.
- Taylor, C. M., Lambin, E. F., Stephenne, N., Harding, R. J., and Essery, R. L. H.: The influence of land use change on climate in the Sahel, *J. Climate*, 15, 3615–3629, 2002.
- Tian, L. and Curry, J. A.: Cloud overlap statistics, *J. Geophys. Res.*, 94, 9925–9935, 1989.
- Tegen, I. and Lacis, A. A.: Modeling of particle size distribution and its influence on the radiative properties of mineral dust aerosol, *J. Geophys. Res.*, 101, 19237–19244, 1996.
- Twomey, S., Piepgrass, M., and Wolfe, T.: An assessment of the impact of pollution on global cloud albedo, *Tellus*, 36B, 356–366, 1984.
- Xue, Y.: Biosphere feedback on regional climate in tropical North Africa, *Q. J. Roy. Meteorol. Soc.*, 123, 1483–1515, 1997.
- Xue, Y. and Shukla, J.: The influence of land surface properties on Sahel climate. Part I: Desertification, *J. Climate*, 6, 2232–2245, 1993.
- Yang, P., Liou, K. N., Wyser, K., and Mitchell, D.: Parameterization of the scattering and absorption properties of individual ice crystals, *J. Geophys. Res.*, 105, 4699–4718, 2000.
- Yang, P., Wei, H., Huang, H.-L., Baum, B. A., Hu, Y. X., Kattawar, G. W., Mishchenko, M. I., and Fu, Q.: Scattering and absorption property database for nonspherical ice particles in the near-through far-infrared spectral region, *Appl. Opt.*, 44, 5512–5523, 2005.
- Yue, Q., Liou, K. N., Ou, S. C., Kahn, B. H., Yang, P., and Mace, G. G.: Interpretation of AIRS data in thin cirrus atmospheres based on a fast radiative transfer model, *J. Atmos. Sci.*, 64, 3827–3842, 2007.
- Yue, X., Wang, H., Liao, H., and fan, K.: Simulation of dust aerosol radiative feedback using the GMOD: 2; Dust-climate interactions, *J. Geophys. Res.*, 115, D04201, doi:10.1029/2009JD012063, 2010.
- Yue, X., Liao, H., Wang, H. J., Li, S. L., and Tang, J. P.: Role of sea surface temperature responses in simulation of the climatic effect of mineral dust aerosol, *Atmos. Chem. Phys.*, 11, 6049–6062, doi:10.5194/acp-11-6049-2011, 2011.
- Yoshioka, M. and Mahowald, N. M.: Impact of desert dust radiative forcing on Sahel precipitation: Relative importance of dust compared to sea surface temperature variations, vegetation changes, and greenhouse gas warming, *J. Climate*, 20, 1445–1467, 2007.
- Zhang, F., Zeng, Q., Gu, Y., and Liou, K. N.: Parameterization of the absorption of H₂O continuum, CO₂, O₂, and other trace gases in the Fu-Liou solar radiation program, *Advances in Atmos. Sci.*, 22, 545–558, 2005.
- Zhao, C., Liu, X., Ruby Leung, L., and Hagos, S.: Radiative impact of mineral dust on monsoon precipitation variability over West Africa, *Atmos. Chem. Phys.*, 11, 1879–1893, doi:10.5194/acp-11-1879-2011, 2011.